Meditation mathematical formalism and Lorentz factor calculation based-on Mindfulness foundation

N. Pornsuwancharoen[a], I.S. Amiri[b], J. Ali[c], P. Youplao[d,e,*], P. Yupapin[d,e,*]

[a] Faculty of Industry and Technology, Rajamangala University of Technology Isan, Sakon Nakhon Campus, Pongkhon, Sakon Nakhon 47160, Thailand
[b] Division of Materials Science and Engineering, Boston University, Boston, MA 02215, USA
[c] Laser Centre, IBNU SINA ISIR, Universiti Teknologi Malaysia, 81310 Johor Bahru, Malaysia
[d] Computational Optics Research Group, Advanced Institute of Materials Science, Ton Duc Thang University, District 7, Ho Chi Minh City 700000, Viet Nam
[e] Faculty of Applied Sciences, Ton Duc Thang University, District 7, Ho Chi Minh City 700000, Viet Nam

ARTICLE INFO

ABSTRACT

Mindfulness foundation is an excellent method of the human spiritual development by the reasonable thinking and consideration, which was established by Lord Buddha a long time ago. There are four ways of thinking and consideration-(i) form (body), (ii) sensation, (iii) spiritual and (iv) Dhamma. In this paper, we propose the use of the form consideration for the spiritual development, in which the form can be considered thoroughly inside the body by the spiritual projection. By using the nonlinear microring resonator known as a Panda-ring resonator, the electromagnetic (EM) signals called polaritons can be generated by the coupling interaction between the intense EM fields and the ionic diploes within the almost closed system, where the dipoles can obtain from the coupling between the gold grating and the strong electromagnetic fields. In the manipulation, cells, tissues, and organs inside the human body can communicate with the spiritual (polaritonic) signals and investigation. The simulation results obtained have shown that the Lorentz factor of 0.99999959 is obtained. The successively filtering of the signal circulation within the body during the meditation can be formulated and the meditation behaviors modeled. The aura, the stopping, and the cold body states can be configured and explained.

Introduction

Mindfulness foundation has been recognized as the most concrete source of thinking in nature, which consists of four foundation thoughts [1,2], which are (i) form (body), (ii) sensation, (iii) spiritual and (iv) Dhamma. Many works in both principles and applications have been reported in the recent literature [3–8]. Some of the studies have attempted the scientific description of mindfulness with some exciting interpretations [9–11], especially, in mathematical formalism and physics. The mindfulness concept is the way of thinking and natural consideration of the spiritual projection into the four foundation principles, where the completion of the four principles is enough to reach the perfect consideration situation. Recently, Ali et al have shown that the polaritonic signals can be generated by using the propagation of the infrared laser injecting into the gold grating embedded within the nonlinear microring resonator [12]. Therefore, the system operation can be considered similar to those in meditation, in which the polariton successive filtering within the body can be realized as the brain signals.

Thus, by considering the generated localized polariton, the brain signals can be manipulated in systems such as the human body. Moreover, various works of the polaritons were also reported [13,14], in which the polaritons were configured as the artificial gauge and quantum current in the investigation. The polariton signal oscillation within the circular-like path can be set up to be the Cerenkov radiation aspect [15,16]. If the equation $1/2\ mv^2 = NK_BT$ satisfied, then the cold system condition is provided, wherein the polariton oscillation can be established within the system [17]. The parameters as m and v are defined as the particle mass and velocity respectively. Here, the number of particles is presented by N, where the Boltzmann constant is K_B and T is the absolute temperature. The frequency tenability of the Rabi oscillation can be performed delicately, where each oscillation frequency has the different energy level. This will require the implementation of a suitable meditation technique, otherwise, the system condition cannot be maintained further, and adverse effects occur. Due to the established conditions, the system noise is negligible, therefore the strength of the polariton field is maximized as a result, the brain performance is very high. In this paper,

the form of consideration is proposed to establish the technique of mathematical formalism, in which the understandable nature can give the mathematical relationship for the form consideration. By considering throughout nature, the understanding details can be linked and formed by the mathematical model. We have proposed the case of study when the brain signals manipulated by the polaritonic signals circulated within the brain like structure. There are 3 cases of the specific phenomenon which are proposed and mathematically interpreted These are (i) the aura situation, (ii) the stopping condition, and the successive filtering aspect, which are discussed in detail in the following sections.

Mathematical formalism

Polaritonic signals generate and propagate within the brain and throughout the human body. The signal within the brain oscillates with the Rabi frequency. It is the same behavior as the active field oscillation in the two-level system [18]. In this proposal, the polaritonic signals can generate within the almost closed system of nonlinear microring system, which is embedded by the gold grating on the center ring, from which the plasmonic island is formed and the coupling is generated between the strong fields and dipoles. The selected light source is an infrared laser, from which the infrared blues shift can be generated, and the aura behavior is obtained. From Fig. 1, the brain signals can generate the polaritonic signals by the coupling strong field and the electrical dipole, which is induced by the intense light pulse within the grating gaps. The system output is realized at the add port which can be derived using the following equations.

$$I_{in} = I_{th} + I_{drop} + I_{add} \qquad (1)$$

where I_{in}, I_{th} and I_{drop} are defined as the input, through and drop port intensities, respectively.

The input intensity is given by

$$E_{in} = E_Z = E_0 e^{-ik_z Z - \omega t + \varphi} \qquad (2)$$

where E_0 is the initial electric field amplitude, k_z is the wave number in the direction of propagation, ω is the angular frequency, where φ is the initial phase.

The add port output of the system in Fig. 1 is given by

$$\mathbf{I_{add}} = -\mathbf{R_{WGM}} \cdot \mathbf{I_{WGMR}} \cdot \mathbf{R_{WGM}} \qquad (3)$$

The material reflectance is defined by $\mathbf{R_{WGM}}$ and as examples, the materials can be gold and TiO_2 [19]. We have used the practically achievable device parameters to perform the system computations
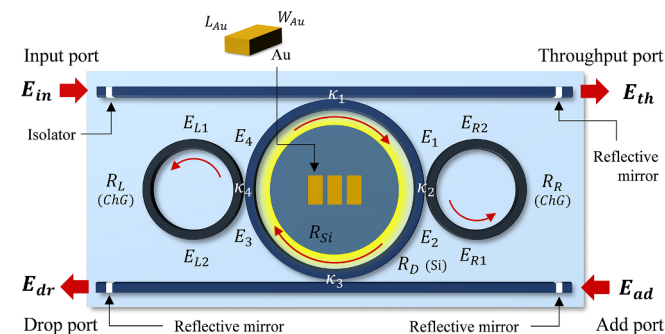
which are given in the figure captions. Fig. 1 shows the reflected output signals from the grating section. In the proposed system, the reflected power is inserted into the Panda-ring system. At the waveguide port the peak reflection is defined as $P_B(\lambda_B) \approx \mathbf{tanh}^2 \left[\frac{N\pi(V)\delta n_0}{n} \right]$ [20]. Here, the number of the periodic variations is defined by N, the waveguide refractive index variation is δn_0 and the fraction of the power within the waveguide is $\pi(V)$, where $\Delta\lambda = \left[\frac{2\delta n_0 \pi}{\pi} \right] \lambda_B$. The Lorentz factor of the red and blue shifts and the center group velocity is given by $\gamma = \left[(1 - \frac{v^2}{c^2})^{1/2} \right]$ [21], where v is the relative velocity between the inertial reference frame, c is the speed of light in vacuum. The blue shift pulse speed is given by $= \lambda\nu$, where ν is the blue shift signal frequency within the system.

Results and discussion

Polaritons can be generated by the coupling between the strong electromagnetic waves and ionic dipoles within the cells or brain cells, which lead to form the quasi-polaritons and propagate within the brain and throughout the body. Generally, they propagate with the speed of light in the medium, which are the plasmonic waves that having the blood contained within the liquid core waveguide (blood vessels). All information can be modulated (demodulated) to (from) the polariton network within the body, in which the communication can be performed between the ionic dipoles and quasi-polaritons. In this work, we are interested in the behaviors of the polariton circulation within the cells (brain cells) with the successively filtering application, which can be manipulated to be the reduction of external noise effect into the system under the meditation. The short pulse in time within the small region (grating pitch) can provide the stronger coupling effect. In the
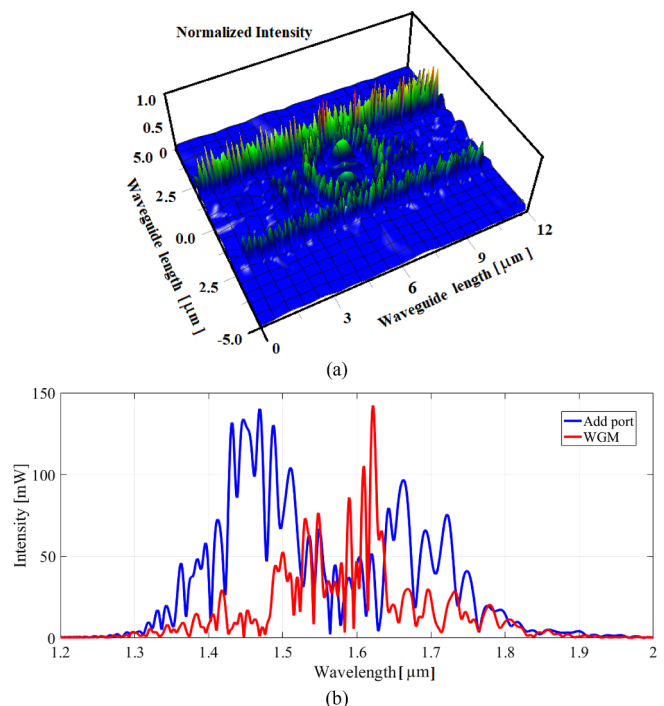

(a)

(b)

Fig. 2. Shows the results of the polariton oscillation distribution in the system in Fig. 1 using the Optiwave program, where the input light pulse power is 15 mW, the center wavelengths is at 1.55 μm. The ring system parameters are $R_L = R_R = 1.20$ μm, $R_D = 1.80$ μm. All κ_1 to $\kappa_4 = 0.5$, the grating pitch is 50 nm. The refractive indices are $n_{0ChG} = 2.90$, the nonlinear refractive index (n_{2ChG}) is 1.02×10^{-17} m² W⁻¹ [22,23], $n_{Si} = 3.47$ (Si, a crystalline silicon). The reflector (TiO_2) dimensions are wide × Length × depth = 0.1 μm × 0.1 μm × 0.2 μm. The used waveguide loss is 0.10 dB cm⁻¹, and the core effective area is 0.30 μm.

Fig. 1. Gold grating embedded in a Panda-ring resonator system model for polariton signals generation, the electrical fields are defined as E_{in}, E_{th}, E_{dr}, E_{ad} representing fields for input, throughput, drop and add ports respectively, the radii of the rings are R_R, R_L, and R_D representing radii for right, left, and the center rings respectively, all coupling coefficients are $\kappa_s = 0.5$ and $\kappa_1–\kappa_4 = 0.5$. R_{Si}: a silicon circle radius, and L_{Au} and W_{Au} are the gold grating dimensions. The parameter of the ring $R_{Si} = 1.80$ μm, R_R and R_L are 1.20 μm, the reflectors (TiO_2) are 0.2–0.5 μm, the gold grating dimensions are 0.1 × 0.1 × 0.2 μm, and the grating pitch is 50 nm.
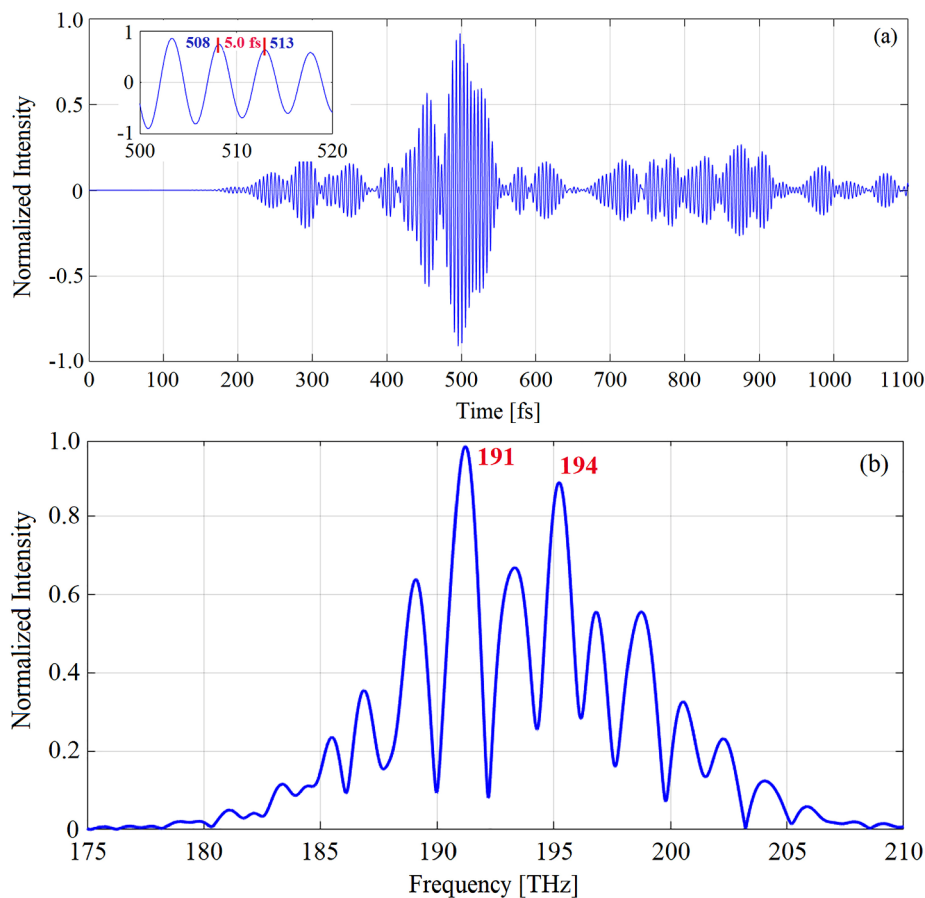
Fig. 3. Shows the results of the polaritonic signal successive filtering output with the 0.1 transmittances obtained at the add port. The input power is 15 mW, where (a) the Rabi oscillation pulse width is 2.60 fs. The inset in (a) is free spectrum range (FSR), which is 5.0 fs, and (b) the Rabi frequencies from the two-level system are at 191 and 194 THz.
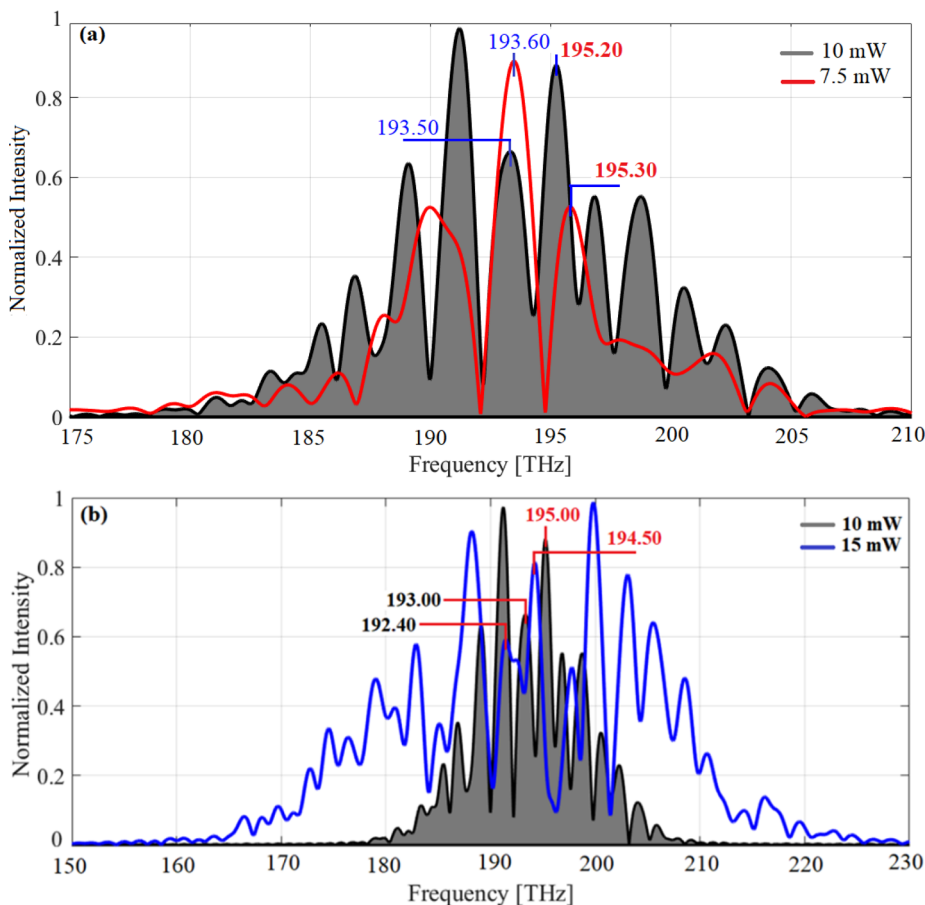

Fig. 4. Shows the plot of the relationship between the normalized intensity and add port output regarding frequency at the add port output. The input powers are 10 and 15 mW, where (a) the redshift signal with the input power are 7.5 and 10 mW, the blue shift signal when the input power is 10 and 15 mW. (For interpretation of the references to colour in this figure legend, the reader is referred to the web version of this article.)

manipulation, the aura state can perform from the blue shift quasi-polaritons, from which the polaritons within the aura band can have the very short pulse width (in time. The blue shift signal propagates faster than the WGM (center) polariton group velocity. In a simulation, there are three aspects of the outputs, which are (i) red and blue shift signals (ii) the stopping in time and (iii) the Lorentz factor, which lead to having the aura, stopping state, and cold body states. The manipulation of such aspects can be formed by the polariton propagation within the circular-like path as shown in Fig. 1, in which the polaritons can generate from the coupling between the WGM light beam and the gold grating. By using the graphical approach called the Optiwave program, the preliminary results are obtained and plotted in Fig. 2, where the related figure captions give the simulation parameters. Polaritonic signals are generated and shown in Fig. 3 regarding relationships between the normalized intensity and time and frequency, respectively. The two-level system generates the center and two-harmonic bands alongside the central group velocity peak signal, which is confirmed by the Rabi oscillation frequency outputs. The results of the polaritonic signal successive filtering output with the 0.1 transmittances obtained at the add port. The input power is 15 mW, where (a) the Rabi oscillation pulse width is 2.60 fs. The inset in Fig. 3 (a) is free spectrum range (FSR), which is 5.0 fs, and (b) the Rabi frequencies from the two-level system are at 191 and 194 THz, where the other tunable frequencies are also seen from 180 to 210 THz. The plot of the relationship between the normalized intensity and add port output regarding

frequency at the add port output is shown in Fig. 4. The input powers are 10 and 15 mW, where (a) the redshift signal with the input power are 7.5 and 10 mW, the blue shift signal when the input power is 10 and 15 mW. The blue and red shift frequencies are 60 and 100 PHz, respectively. The plot of the relationship between the polariton successive oscillation time and internal energy (input power), which is varied from 1 to 10 mW, where (a) the overall output signals, and (b) the add port relative signal between the WGM (center signals) and the blue shift signals. The curve fitting is applied, where the simulation data are the square and circle colors). The minimum oscillation pulse width between 2.0 and 2.35 fs is obtained, which can give the lack in time between the center group velocity peak and the blue shift signals of 194 THz (0.19 PHz). From which the calculation Lorentz factor of 0.99999959 is obtained. The change in the time of the pulse at the WGM and the blue shift are plotted, from which the strong coupling leads the increase in the relative time between the center group velocity and the blue shift signals. The successive filtering for a long time can give the very short aura signal pulse width ($\Delta t \to 0$), which is called the stopping state [17]. The cold state is also seen, while the Lorentz factor can also be calculated (Fig. 5.).

Conclusion

We have proposed the compelling concept of the meditation, which can be configured by the mathematical formalism. The meditation
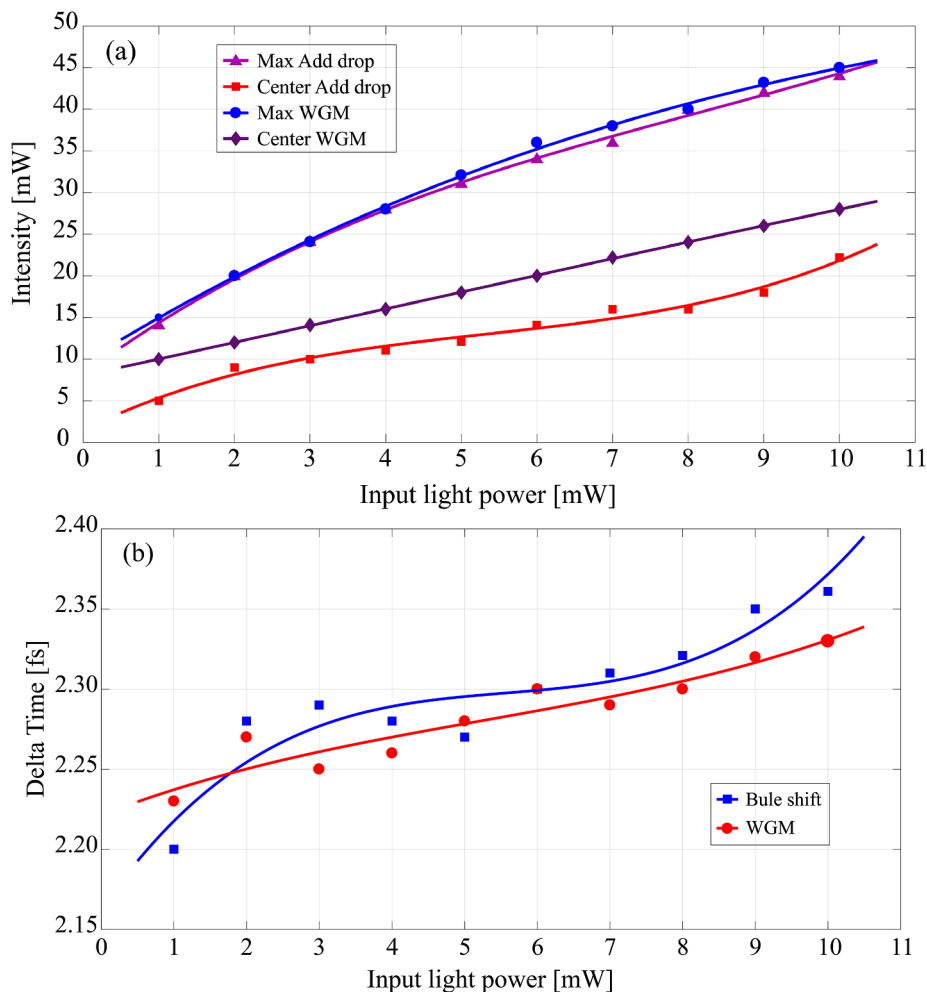

Fig. 5. Shows the plot of the relationship between the polariton successive oscillation time and internal energy (input power), which is varied from 1 to 10 mW, where (a) the overall output signals, and (b) the add port relative signal between the WGM (center signals) and the blue shift signals. The curve fitting is applied, where the simulation data are the square and circle colors). (For interpretation of the references to colour in this figure legend, the reader is referred to the web version of this article.)

states and behaviors can be configured and described convincingly. The polaritonic signals generated by the microring embedded a gold grating within the device called a Panda-ring resonator. A closed polaritonic signal configures the manipulation system closed system, where the polariton energy is kept within the closed system similar to one Mindfulness Foundation principles during the meditation, which can be formed by the selected reflector length (TiO_2). By using the infrared light source input, the results obtained have shown that the three significant occurrences such as the aura, stopping and cold body states can be explained. **Answer**: The blue shift signal has occurred during the meditation due to the successive filtering, which is the aura state. From which the shift between the polaritonic center and the blue shift signals is calculated and found. The stopping condition has occurred when the change in time of the blue shift signal is approached zero, where $1/2\ mv^2 = NK_BT$, the cold state with T = 0 is obtained. Moreover, the blue shift signals can be used to explain the lack in time between the two relative frames, which are the center group velocity and the aura state signals. By using the Lorentz factor calculation, the factor of 0.99999959 is obtained, which means that the material under the aura state can have the present time less than the reverence frame. The more explanation of the cold body when the time(pulse width) of the aural signal is approached zero, quantum conscious and restoring ageing can also be explained, which will be the continuous works.

Acknowledgment

Appendix A. Supplementary data

Supplementary data to this article can be found online at https://doi.org/10.1016/j.rinp.2018.11.005.

References

[1] Edelglass W, Garfield J. Buddhist philosophy: essential readings. Oxford University Press; 2009.

[2] Yupapin PP. Buddhism and quantum physics: generality. Int J Sci World 2015;3:221–2.

[3] Greenberg MT, Mitra JL. From mindfulness to right mindfulness: the intersection of awareness and ethics. Mindfulness 2015;6:74–8.

[4] van den Hurk PA, Wingens T, Giommi F, Barendregt HP, Speckens AE, van Schie HT, et al. the relationship between the practice of mindfulness meditation and personality—an exploratory analysis of the mediating role of mindfulness skills. Mindfulness 2011;2:194–200.

[5] Wheeler MS, Arnkoff DB, Glass CR. The neuroscience of mindfulness: how mindfulness alters the brain and facilitates emotion regulation. Mindfulness 2017;8:1471–87.

[6] Bergomi C, Tschacher W, Kupper Z. Meditation practice and self-reported mindfulness: a cross-sectional investigation of meditators and non-meditators using the comprehensive inventory of mindfulness experiences (CHIME). Mindfulness 2015;6:1411–21.

[7] Evans K, Vasquez E. Mindfulness based stress reduction and citizenship education: a systemic review of the empirical literature. Mindfulness Compassion 2017;2:159–69.

[8] Van Gordon W, Shonin E, Lomas T, Griffiths MD. Corporate use of mindfulness and authentic spiritual transmission: competing or compatible ideals? Mindfulness Compassion 2016;1:75–83.

[9] Heredia L, Gasol L, Ventura D, Vicens P, Torrente M. Mindfulness-based stress reduction training program increases psychological well-being, and emotional regulation, but not attentional performance. A pilot study. Mindfulness Compassion 2017;2:130–7.

[10] Tang Y-Y, Hölzel BK, Posner MI. The neuroscience of mindfulness meditation. Nat Rev Neurosci 2015;16:213215.

[11] Ricard M, Lutz A, Davidson RJ. Mind of the meditator. Scientific American 2014;311:38–45.

[12] Ali J, Pornsuwancharoen N, Youplao P, Amiri I, Poznanski R, Chaiwong K, et al. Characteristics of an on-chip polariton successively filtered circuit. Results Phys 2018;11:410–3.

[13] Lim H-T, Togan E, Kroner M, Miguel-Sanchez J, Imamoğlu A. Electrically tunable artificial gauge potential for polaritons. Nat Commun 2017;8:14540.

[14] Matsuura H, Wasaki K. Quantization of artificial neuron (quantum current, model of polariton on axon). Int J Innovative Comput Inf Control 2014;10:1121–33.

[15] Yupapin P, Thammawongsa N, Ali J. Consciousness and subconsciousness detection model under Čerenkov radiation. Microwave Opt Technol Lett 2014;56:1584–7.

[16] Jomtarak R, Yupapin PP. Multi-wavelength Čerenkov radiations in a microring resonator in combination with two gratings. Optoelectron Lett 2015;11:252–5.

[17] Yupapin PP, Pornsuwancharoen N. Proposed nonlinear microring resonator arrangement for stopping and storing light. IEEE Photonics Technol Lett 2009;21:404–6.

[18] Youplao P, Pornsuwancharoen N, Amiri I, Jalil M, Aziz M, Ali J, et al. Microring stereo sensor model using Kerr-Vernier effect for bio-cell sensor and communication. Nano Commun Networks 2018;17:30–5.

[19] Pornsuwancharoen N, Jalil MA, Amiri IS, Ali J, Yupapin P. Dual mode grating sensor using microring conjugate mirror and plasmonic island. Microwave Opt Technol Lett 2018;60:2595–9.

[20] Gupta P, Ramakrishna SA, Wanare H. Strong coupling of surface plasmon resonances to molecules on a gold grating. J Opt 2016;18:105001.

[21] Moradpour H, Bahadoran M, Youplao P, Yupapin P, Ghasemi A. One and two spin-1/2 particle systems under the Lorentz transformations. J King Saud Univ-Sci 2017;30(4):506–12.

[22] Atabaki AH, Moazeni S, Pavanello F, Gevorgyan H, Notaros J, Alloatti L, et al. Integrating photonics with silicon nanoelectronics for the next generation of systems on a chip. Nature 2018;556(7701):349–54.

[23] Smektala F, Quemard C, Leneindre L, Lucas J, Barthélémy A, De Angelis C. Chalcogenide glasses with large non-linear refractive indices. J Non-Cryst Solids 1998;239:139–42.